# Supporting Information

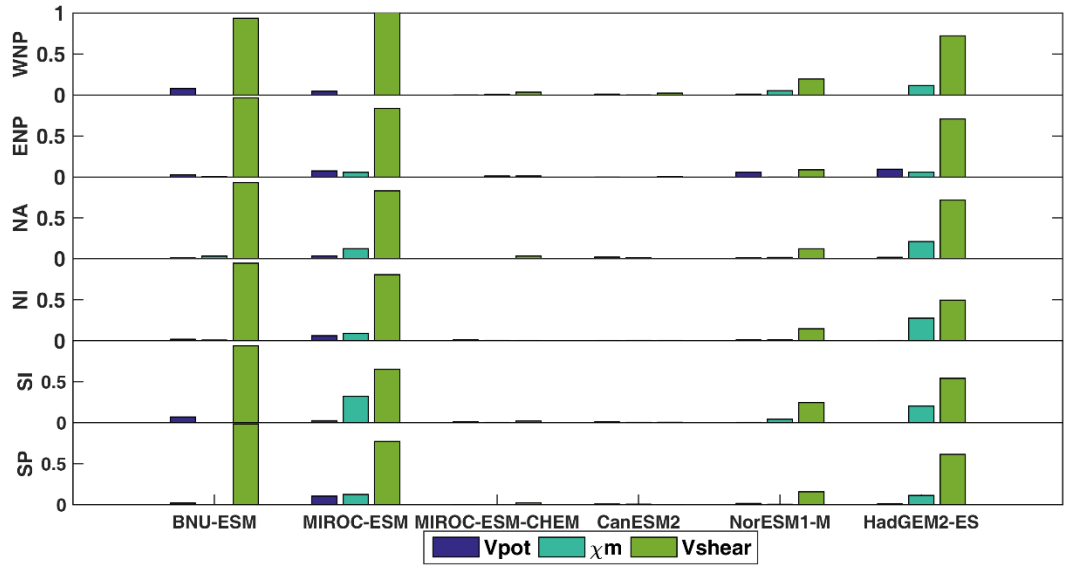


**Figure S1**. The fractional variance contribution of components of VI during the TC season and within the six TC basins during 2040-2069.

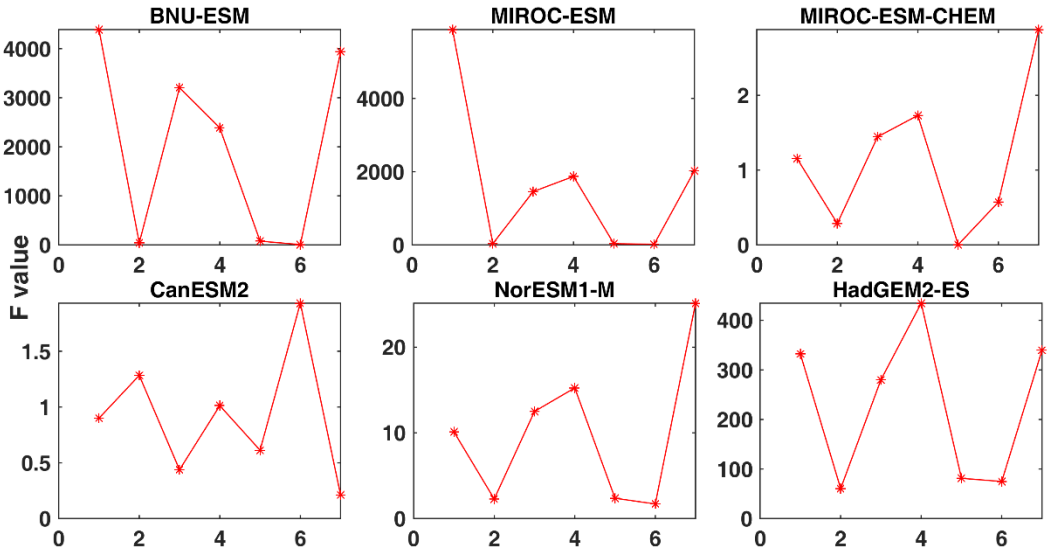


**Figure S2.** The F-statistic of the 7 different combinations of regression variables for VI differences between G4 and RCP4.5. The x-axis on each panel represents the combination of components used as predictors in each regression equation:

1:($V_{pot}$, $V_{shear}$, $\chi_m$), 2:($V_{pot}$, $V_{shear}$), 3:($V_{pot}$, $\chi_m$), 4:($V_{shear}$, $\chi_m$), 5:($V_{pot}$), 6:($\chi_m$), 7:($V_{shear}$).

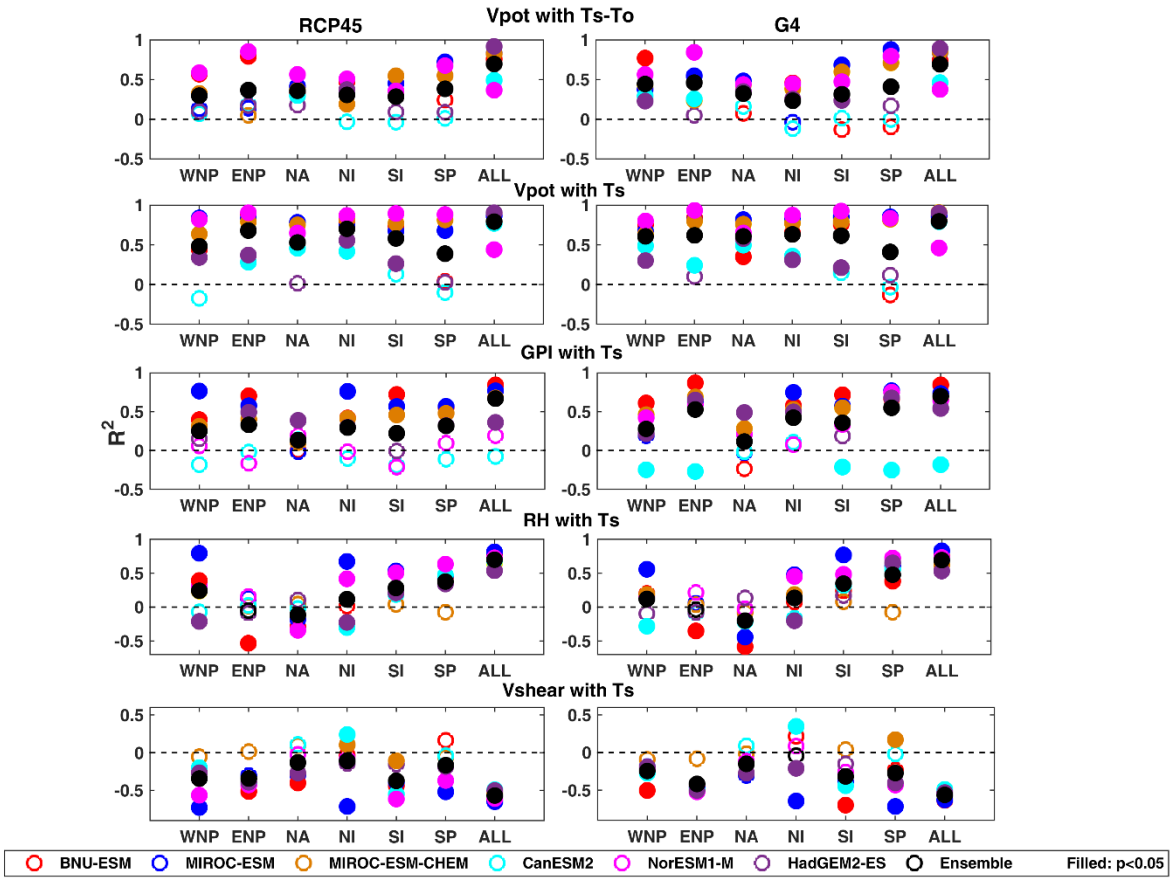


**Figure S3**. The correlations ($R^2$) between variable fields in RCP4.5 (left column), and G4 (right column) separately for comparison with Fig. 7. Top to bottom $V_{pot}$ anomalies as a function static stability $T_S$ - $T_O$; sea surface temperature differences ($T_S$) and: $V_{pot}$, GPI, relative humidity, and vertical wind shear. Data is during TC season and across the six TC basins for the years 2040-2069. Each model is weighted equally in the ensembles regardless of number of observations.

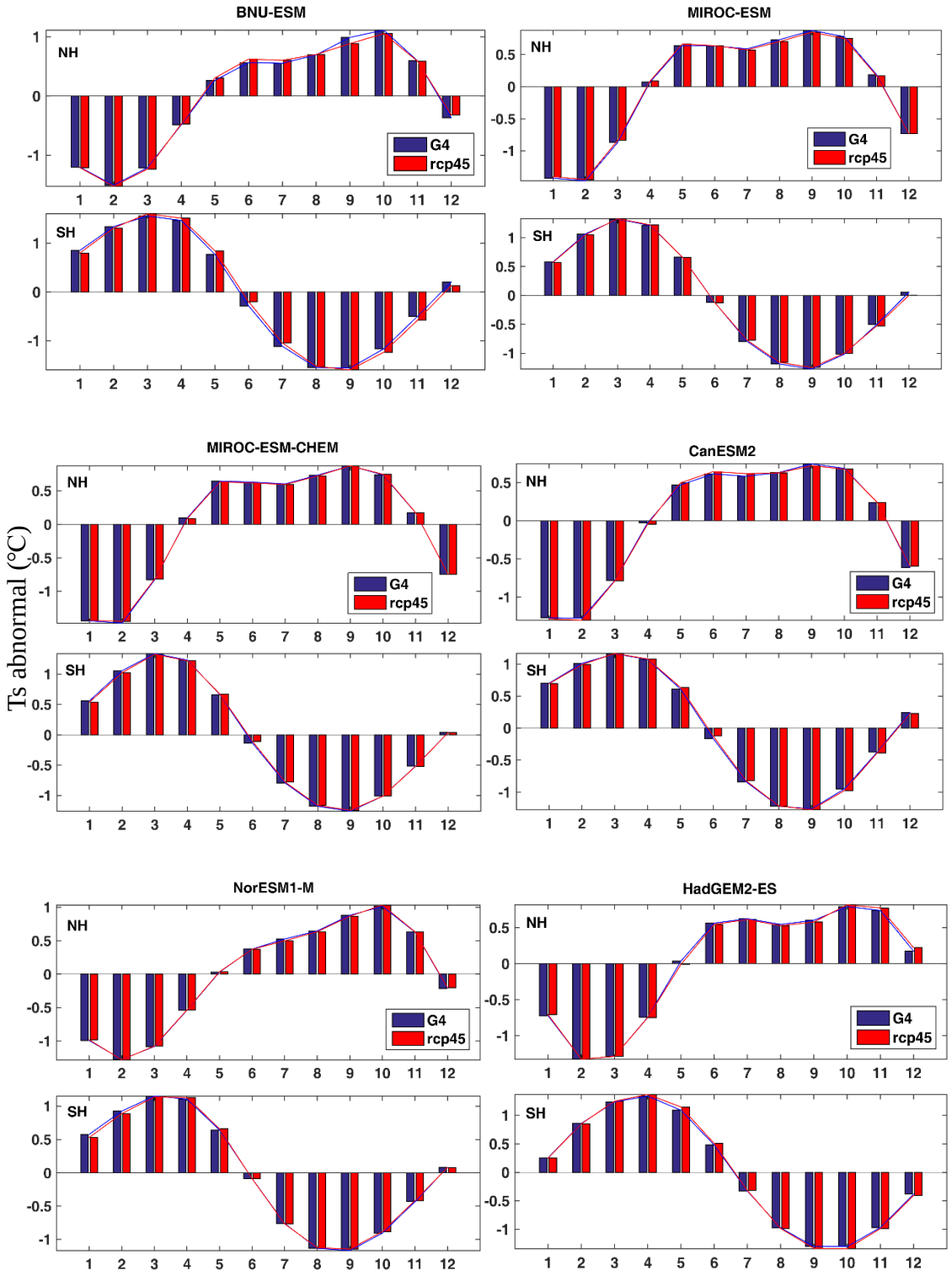


**Figure S4**.The seasonal of $T_s$ during 2040-2069 in northern and southern hemisphere TC basins.

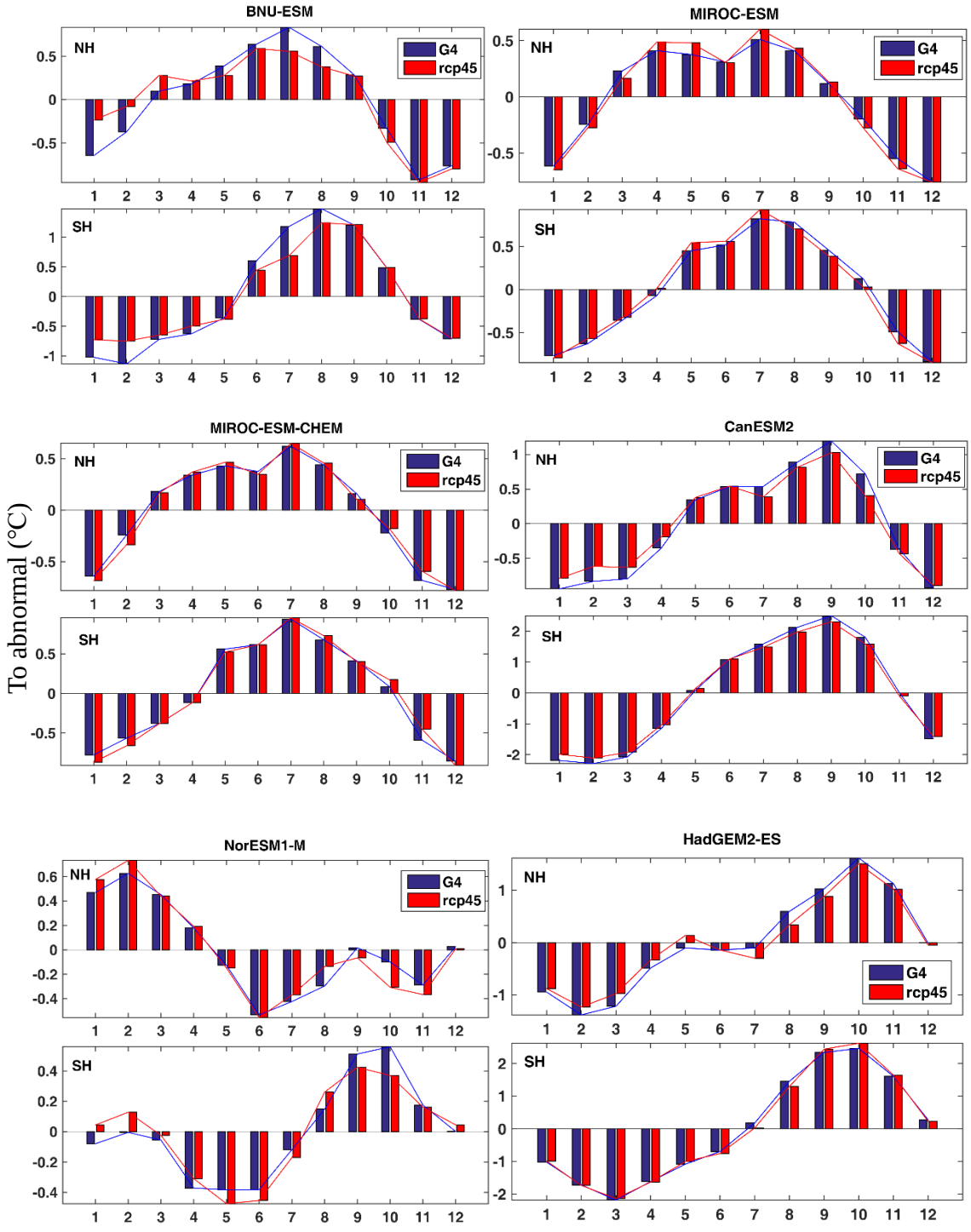


**Figure S5.** The seasonal cycle of $T_0$ (100hPa) during 2040-2069 in northern and southern hemisphere TC basins.

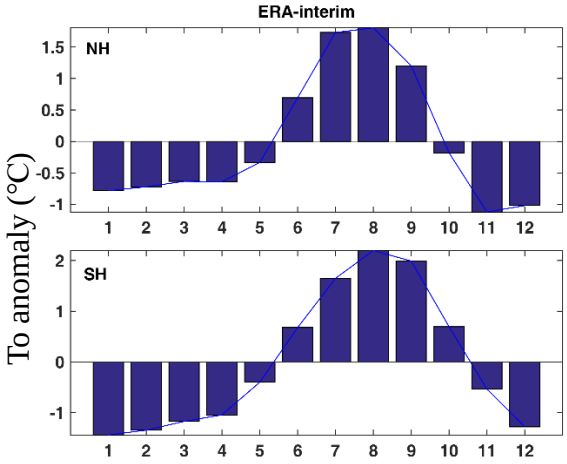


**Figure S6.** The seasonal cycle of $T_0$ (100hPa) in northern and southern hemisphere TC basins from ERA-interim for 1987-2016.

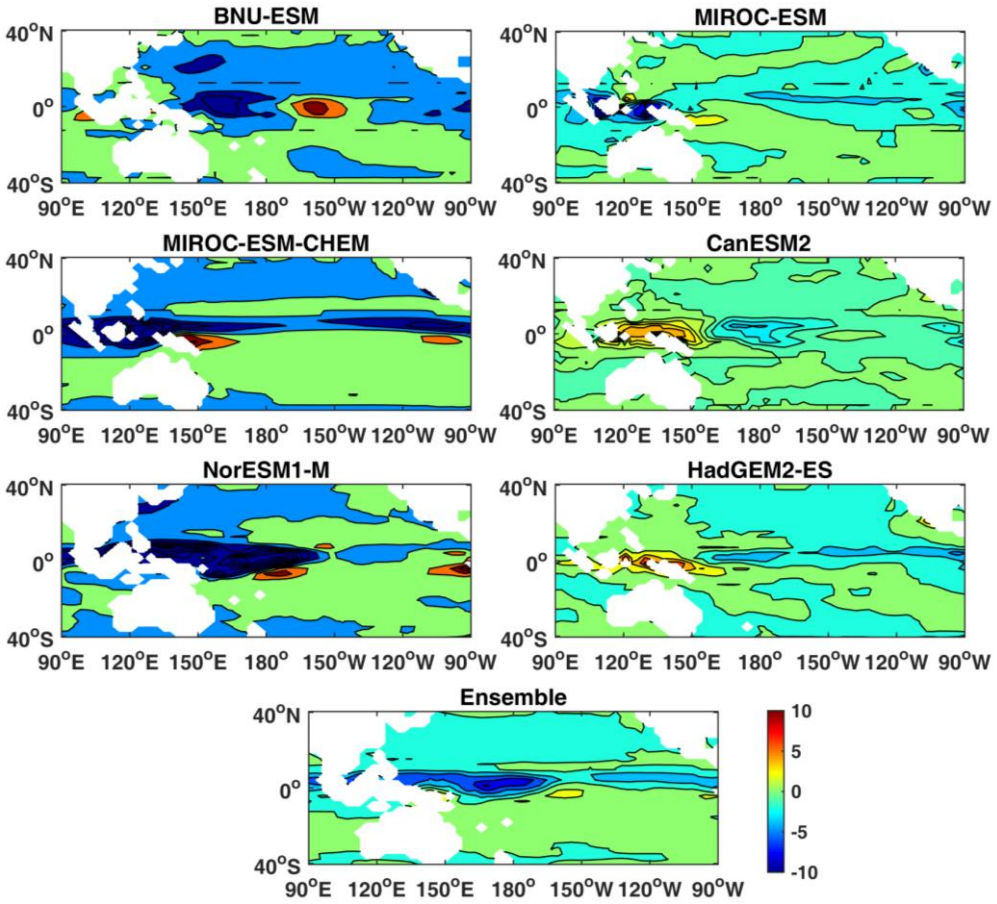


Fig. S7. GPI difference (G4-RCP4.5) for the years 2040-2069, over the Pacific Ocean.